International Research Journal of Advanced Engineering and Science
ISSN (Online): 2455-9024

Simulation of 3 Phase Train Drive Traction Motor Control System for Developing Green Energy Technology and Improving Train Drive System Performance

R. Akbar Nur Apriyanto[1], Mohammad Erik Echsony[2], R. Gaguk Pratama Yudha[3], Adiratna Ciptaningrum[4], Wahyu Pribadi[5], Rahayu Mekar Bisono[6], Dwi Adhim Zuhli Atmaja[7]
[1, 2, 3, 4, 5, 6, 7]Department of Engineering, Madiun State Polytechnic, Jl. Serayu No. 84, Pandean, Taman, Pandean, Kec. Taman, City of Madiun, East Java 63133

Abstract**—***In Vector Control there are two stator current settings, d-axis and q-axis. The d-axis and q-axis stator currents have an impact on the performance of the induction motor. Controlling the d-axis and q-axis can use the PID controller, but it is difficult to determine the values of Kp, Ki, and Kd. The Particle Swarm Optimization algorithm can find the optimal value from several groups. In this paper, a method for controlling the performance of an induction motor with the d-axis stator current method will be given using a PID controller that is optimized with the Particle Swarm Optimization (PSO) algorithm based on LabView as system validation. The evaluation that will be observed is the performance of the induction motor with a varying load testing scheme at nominal speed. From the two tests of d-axis stator current controller using PSO algorithm PID and PID without PSO algorithm, PID-PSO produces good speed performance and is able to reduce phase current consumption, d-axis stator current ripple and phase current THD compared without PID-PSO. Thus, PID-PSO obtained an efficiency of 89.02% at nominal speed and a load of 5 Nm.*

Keywords**—** *LabView; Induction Motor; Particle Swarm Optimization; Vector Control*

I. INTRODUCTION

Controlling the speed of an induction motor according to the needs is very difficult because the induction motor is designed to work at a nominal speed, thereby changing the construction of the motor. Induction motor control is divided into two methods: scalar control and vector control. Scalar control was used in several study literature because it has many advantages, one of which is that it is easier to design and implement (Apriyanto et al. 2020). In this method, the significant advantage is that induction motors do not require parameters (Reza, Islam, and Mekhilef 2014; Suetake, Da Silva, and Goedtel 2011).

Vector control has advantages: good efficiency and high dynamic performance (Braslavsky et al. 2006; Ferdiansyah et al. 2018). Flux and torque are important components in vector control because they are able to adjust separately like separate amplifier direct current motors (Purwanto et al. 2014).

Reasonable speed performance at vector control is generated by controlling current, speed, flux, and torque. There are two settings on vector control, i.e., the dq-axis stator current setting (Briz et al. 2001). Stator current setting d-control variable axis for rotor flux, and stator current setting q-variable axis control for torque. Vectors of current, flux, and voltage dq-axis will form a model of stator phase currents in induction motors (Quang et al. 2015). The correlation of stator current setting performance dq-axis will affect the trend of speed response and phase current performance in induction motors. Especially in current settings, the d-axis affects the speed efficiency of induction motors. (Bazzi et al. 2010)

Particle Swarm Optimization (PSO) is the newest method discovered in 1995 by Eberhart and Kennedy. PSO is inspired by the way birds flock. This method promises an uncomplicated implementation but is reliable (Ramli et al. 2015). The working principle of this algorithm is to look for PID parameters that pass from the local group. After that, from the results that pass from the local group, the most optimal is selected to make the optimal locale. Then, local optimal from many groups will be filtered to global optimal (Salem, Awadallah, and Bayoumi 2015).

LabView is a supported virtual instrument monitoring regular real-time data acquisition. LabView excels at building user interfaces with easy graphical programming (A 2016; Nhizanth and Gopalakrishnan 2015). LabView supports hardware such as a National Instrument product called MyRIO in its implementation. By using MyRIO, it will be easy to implement motor speed data acquisition automatically in real-time due to the reliability and FPGA-based signal processing capabilities that MyRIO has.

This paper discusses the performance of induction motors with the method vector control stator current setting d-axis that uses a PID controller, where the parameter values of Kp, Ki, and Kd are obtained from automatic tuning of the PSO algorithm. The PSO algorithm PID controller will conduct the testing mechanism, namely testing the load varies with nominal speed. The validation of this paper is carried out through a LabView simulation.

This study aims to enrich LabView's research in Indonesia. In particular, this study observed the effect of setting the d-axis stator current on the performance of a 3-phase induction motor with a PID controller, in which the values for the parameters Kp, Ki, and Kd have been optimized using an algorithm Particle Swarm Optimization (PSO).

R. Akbar Nur Apriyanto, Mohammad Erik Echsony, R. Gaguk Pratama Yudha, Adiratna Ciptaningrum, Wahyu Pribadi, Rahayu Mekar Bisono, and Dwi Adhim Zuhli Atmaja, "Simulation of 3 Phase Train Drive Traction Motor Control System for Developing Green Energy Technology and Improving Train Drive System Performance," *International Research Journal of Advanced Engineering and Science*, Volume 8, Issue 4, pp. 33-40, 2023.

International Research Journal of Advanced Engineering and Science
ISSN (Online): 2455-9024

II. WRITING METHOD

A. Vector Control

Representation of a coordinate system dq-axis is the induction motor current assembled from a complex vector. The combination of currents can be the stator current vector, which rotates at a specific frequency as in (1) and is illustrated in Figure 1.

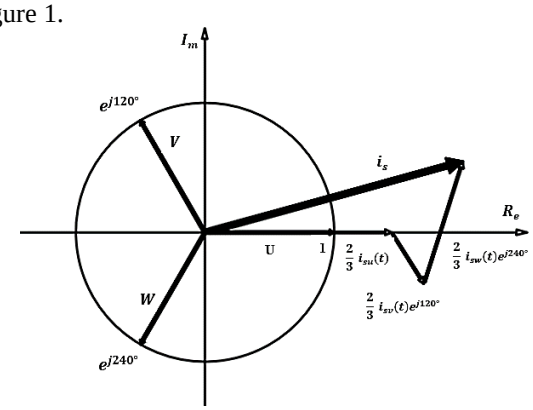

Fig. 1. Stator current vector.

$$i_s = \frac{2}{3}\left[i_{su}(t) + i_{sv}(t)\,e^{j\frac{2\pi}{3}} + i_{sw}(t)\,e^{j2\left(\frac{2\pi}{3}\right)}\right] \quad (1)$$

Value combination magnitude three phases will form a coordinate system of dq-axes that rotate synchronously. Magnitude The three phases are divided into two components, d and q. equality magnitude current, flux linkage and voltage are expressed in equations (2), (3), and (4).

$$u_s = u_{ds} + ju_{qs};\ u_r = u_{dr} + ju_{qr} \quad (2)$$

$$i_s = i_{ds} + ji_{qs};\ i_r = i_{dr} + jr_{qr} \quad (3)$$

$$\lambda_s = \lambda_{ds} + j\lambda_{qs};\ \lambda_r = \lambda_{dr} + j\lambda_{qr} \quad (4)$$

From equations (2), (3), and (4), finally, there is the concept that an induction motor can be linearized and treated like a separate amplifier direct current motor (Purnata et al. 2015; Purwanto et al., 2011). Figure 2 is the working principle of vector control.

In the process of Vector control, there are four signal feedbacks, namely the rotor speed (ω_r) obtained from the speed sensor installed as feedback speed control will produce a torque reference output (T_e^*). Control Signal as input for stator current reference q-axis (i_{qs}^*) equation (5) plus the flux estimation result ($Phir$) of (6) and calculation of slip velocity (7). Stator current reference value d-axis (i_{ds}^*) is very important for a constant d-axis current scheme.

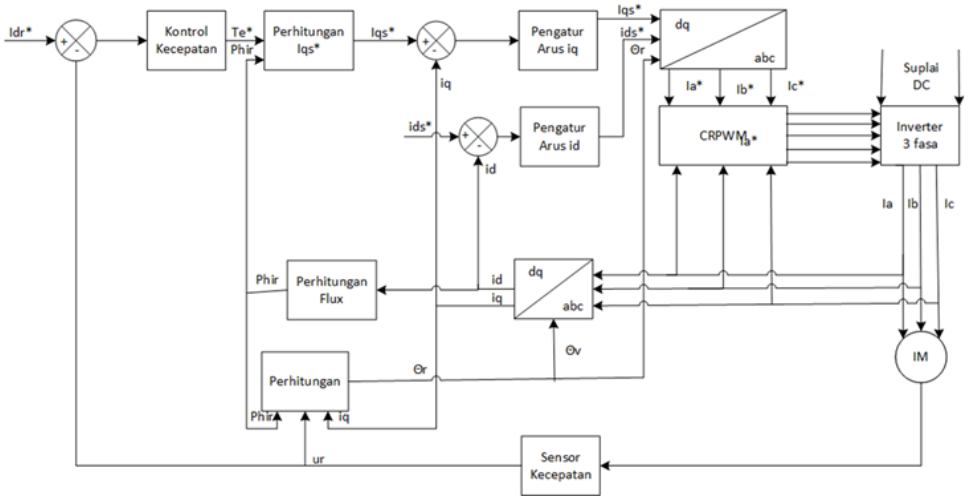

Fig. 2. Working block

$$i_{qs}^* = \frac{2}{3}.\frac{2}{P}.\frac{L_r}{L_m}.\frac{T_e^*}{|\lambda_r^*|} \quad (5)$$

$$|\lambda_r| = \frac{L_m.i_{ds}}{1+\tau_r s} \quad (6)$$

$$\omega_{sl} = \frac{L_m}{\lambda_r^*} * \frac{R_r}{L_r} * i_{qs}^* \quad (7)$$

Stator phase current sensor reading as Three other feedback signals. Then, there was a Clark-Park transformation, where three feedback signals were transformed into dq-axis currents. This paper uses the scheme of indirect vector control to determine the transformation coordinates by equation (8) (Hussain & Bazaz, 2015).

The Clark transformation can be expressed in equations (9) (10) on the conversion stationary frame.

$$\theta_e = \int (\omega_m + \omega_{sl})\,dt \quad (8)$$

$$i_\alpha = i_a \quad (9)$$

$$i_\beta = \frac{1}{\sqrt{3}}\,i_a + \frac{2}{\sqrt{3}}\,i_b \quad (10)$$

The Park transformation is expressed in equations (11) and (12) on the conversion rotating frame.

$$i_{ds} = i_\alpha.\cos(\theta) + i_\beta.\sin(\theta) \quad (11)$$

$$i_{qs} = -i_\alpha.\sin(\theta) + i_\beta.\cos(\theta) \quad (12)$$

In the input of the 2 inner loops, the control currents of the stator are obtained by subtracting the transformed stator

R. Akbar Nur Apriyanto, Mohammad Erik Echsony, R. Gaguk Pratama Yudha, Adiratna Ciptaningrum, Wahyu Pribadi, Rahayu Mekar Bisono, and Dwi Adhim Zuhli Atmaja, "Simulation of 3 Phase Train Drive Traction Motor Control System for Developing Green Energy Technology and Improving Train Drive System Performance," *International Research Journal of Advanced Engineering and Science*, Volume 8, Issue 4, pp. 33-40, 2023.

International Research Journal of Advanced Engineering and Science
ISSN (Online): 2455-9024

currents in the dq-axis from the reference stator currents in the dq-axis. The performance of the induction motor controlled by vector control relies on these inner loops (Briz et al., 2015). Meanwhile, the outputs of the 2 inner loops for stator current control (i''_{ds} and i''_{qs}) serve as inputs to the inverse Clark-Park transformation (13), (14). Equations (15), (16), (17) are for the inverse Clark transformation only.

$$i_\alpha = i''_{ds}.\cos(\theta) - i''_{qs}.\sin(\theta) \quad (13)$$

$$i_\beta = i''_{ds}.\sin(\theta) + i''_{qs}.\cos(\theta) \quad (14)$$

$$i_a = i_\alpha \quad (15)$$

$$i_b = -\frac{1}{2} i_\alpha + \frac{\sqrt{3}}{2} i_\beta \quad (16)$$

$$i_c = -\frac{1}{2} i_\alpha - \frac{\sqrt{3}}{2} i_\beta \quad (17)$$

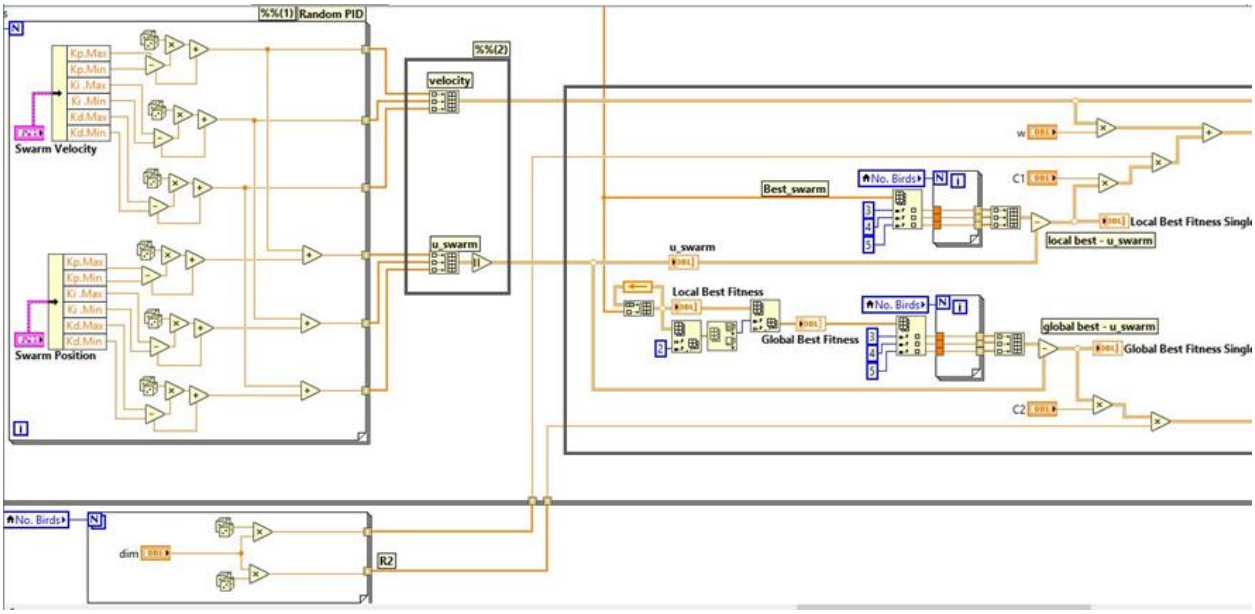

Fig. 3. PID parameter tuning with PSO on LabView.

The current regulator PWM (CRPWM) inverter requires a stator current reference obtained from the Clark-Park transformation output. The inverter is an induction motor control by adjusting the frequency and magnitude of the three-phase signal.

B. PID-Particle Swarm Optimization (PID-PSO)

PSO is a recent computational technique discovered by Ebehart and Kennedy in 1995. PSO draws inspiration from how birds flock together (Fakhruddin et al., 2020). Each particle's position can be considered a candidate solution for an optimization problem. Each particle is assigned a fitness function tailored to the corresponding problem.

Particles in PSO occupy two positions: the first position is the best point within a group or iteration (local best). In contrast, the second position is the best point across all iterations (global best). The PSO algorithm relies on two factors: velocity and position of the particles. These factors can be updated using Equations (18) and (19).

$$V_i^d(t+1) = wV_i^d(t) + c_1 r_1 \left(P_i^d(t) - X_i^d(t)\right) + c_2 r_2 \left(P_i^d(t) - X_i^d(t)\right) \quad (18)$$

$$X_i^d(t+1) = X_i^d(t) + V_i^d(t+1) \quad (19)$$

Where c_1 and c_2 are the respective rates of social change; r_1 and r_2 are random values between 0 and 1; V is the individual's velocity factor i at iteration d; t is the current iteration; is the inertia weight; and X is the position factor.

PSO has the advantage of converging to central patterns and the ability to solve complex optimization problems in various domains. The limitation of PSO is its susceptibility to getting trapped in local optima, and if there are errors in selecting parameters, the results will not be satisfactory (Chao et al., 2015).

The PID method is a conventional method with perfect results. PID is a combination of gain Proportional (P), Integral (I), and Derivative (D). This combination serves to cover deficiencies and maintain the advantages of each character. The PID method is an equation sensitive to system transfer function changes.

Therefore, the PID method is often combined with other methods to tune automatically (Ali et al., 2014). In this research, PID parameters will be tuned offline using PSO. So, equations 2 and 3 apply to each value of Kp, Ki, and Kd, as shown in Figure 3 on LabView. After that, parameters Kp, Ki, and Kd optimization continued, as in Figure 3, to find the Global Best.

III. RESULT AND DISCUSSION

A. Simulation Design in LabView

LabView is used in this paper for a simulation project

R. Akbar Nur Apriyanto, Mohammad Erik Echsony, R. Gaguk Pratama Yudha, Adiratna Ciptaningrum, Wahyu Pribadi, Rahayu Mekar Bisono, and Dwi Adhim Zuhli Atmaja, "Simulation of 3 Phase Train Drive Traction Motor Control System for Developing Green Energy Technology and Improving Train Drive System Performance," *International Research Journal of Advanced Engineering and Science*, Volume 8, Issue 4, pp. 33-40, 2023.

International Research Journal of Advanced Engineering and Science
ISSN (Online): 2455-9024

aimed at automating PID tuning using PSO. In the simulation project, the user interface is designed as depicted in Figure 4, with each panel serving various functions.

The green-colored panel, indicated by circle 1, represents the initial settings of PSO. This green-colored panel includes the range of values for Kp, Ki, and Kd (referred to as swarm position), the range of changes for Kp, Ki, and Kd (referred to as swarm velocity), the number of birds in one group (referred to as number of birds), the number of groups in one population (referred to as Bird Step), C1 and C2 are the rate of social change, inertia weight value or w, dimension value or dim. The automatic tuning method with PSO can be used by activating the PSO switch to ON.

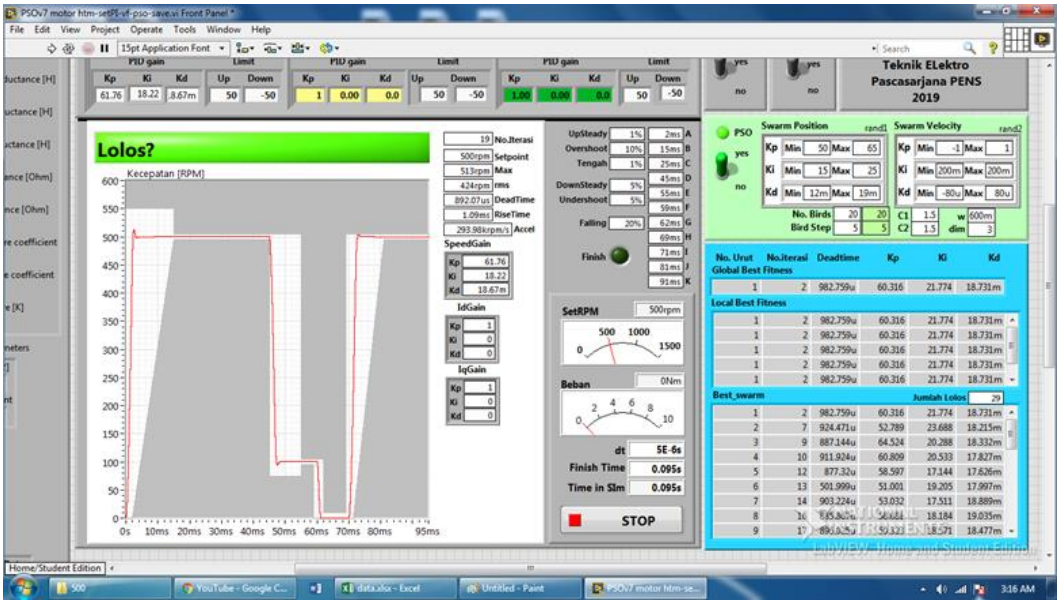

Fig. 4. Display of the PID algorithm PID simulation results.

Circle 2 stores the rules/systematic performance of the system to be achieved. It is declared passed when the PID parameter produces maximum system performance (red line) running on the white line. Rules/systematic performance consists of error steady maximum when the reference speed (written UpSteady in percent), overshoot maximum (written Overshoot in percent), error steady maximum when the speed is slowed down to 20% of the reference (write down the Middle in percent), error steady maximum when the speed is slowed down to 0 Rpm (written DownSteady in percent), undershoot maximum when the reference speed is reduced by 20% from its initial value (written Undershoot in percent), and how many percent decrease in reference speed (write down Falling in percent).

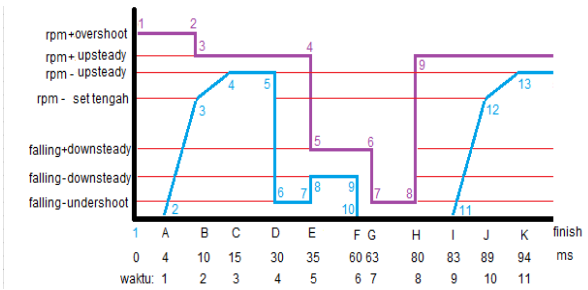

Fig. 4. The position of the A-K variable timing in the simulation.

As for the letters A-K in circle 3 are performance rules in time (in milliseconds). This timing is related to determining several rules, such as determining the maximum dead time, rise time, steady time, and falling time. More details, details of the timing scheme are in Figure 5.

TABLE I. PSO Parameter Value Criteria

No.	Description	Value
1.	Time	=100ms
2.	Discrete Time (d_t)	=5e-6s
3.	Dead Time (t_d)	<=10ms
4.	Rise Time	Deadtime+10ms
5.	Middle	<=15ms, <=Setpoint-20%
6.	Overshoot	<=Setpoint±2%
7.	Steadystate(s_t)	<=Setpoint±2%

The blue-colored panel within circle 4 represents a table containing values of particles resulting from automated PSO-PID analysis that passes the learning phase. Particles that pass in a group of parameters are recorded in the "best swarm" table, the recorded parameters include serial number, iteration, dead time, Kp, Ki, and Kd. The "local best fitness" table stores the best individuals from each respective group. The "global best fitness" table represents the best individuals from the whole group in the population. The parameters of the global best fitness represent the PID parameters that have been optimized using the PSO algorithm. The determination of the best individual is based on the largest dead time parameter, which is grounded in the response during loading. When the shortest dead time is used, there can be a delay in the motor's starting time when a load is applied. This inconsistent delay

R. Akbar Nur Apriyanto, Mohammad Erik Echsony, R. Gaguk Pratama Yudha, Adiratna Ciptaningrum, Wahyu Pribadi, Rahayu Mekar Bisono, and Dwi Adhim Zuhli Atmaja, “Simulation of 3 Phase Train Drive Traction Motor Control System for Developing Green Energy Technology and Improving Train Drive System Performance,” *International Research Journal of Advanced Engineering and Science*, Volume 8, Issue 4, pp. 33-40, 2023.

must be avoided when designing motor control that prioritizes comfort, such as electric vehicles.

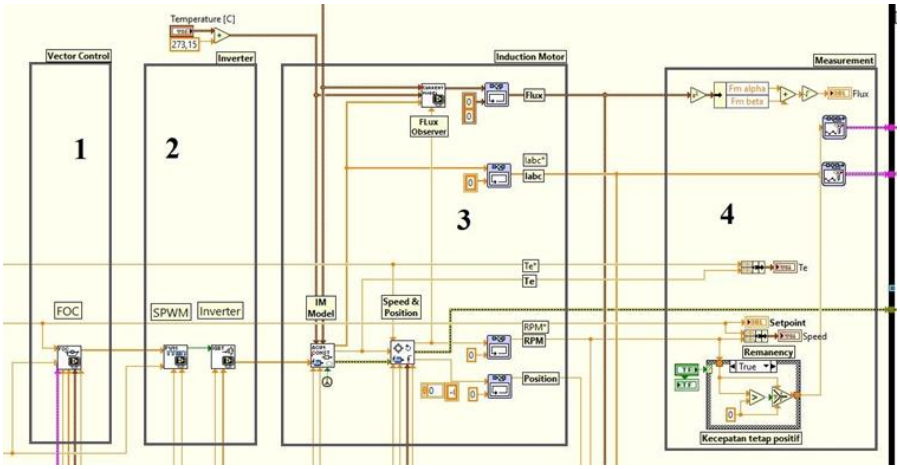

Fig. 6. LabView simulation

In circle 5, "SetRPM" is the reference speed input (in RPM) that the PID parameters aim to achieve. According to this test, the load is kept constant at 0 Nm (no load), and the simulation duration being discussed/analyzed for tuning is 95 milliseconds (Finish Time). In circles 6 & 7, "PID Id" and "PID Iq" are parameters in vector control.

Figure 6 represents a block diagram of the simulation in LabView. The diagram above has several sections: 1. FOC Block, 2. 3-Phase Inverter Control Block, 3. 3-Phase Induction Motor Subprogram, 4. Measurement Device Subprogram.

TABLE II. Parameters of 3-Phase Induction Motor

No.	Parameter	Value	Unit
1.	R_{stator}	5.27	*Ohm*
2.	R_{rotor}	3.40	*Ohm*
3.	L_{stator}	4.33	*mH*
4.	L_{rotor}	4.46	*mH*
5.	$L_{maqnetization}$	270	*mH*
6.	P_n	1.5	*HP*
7.	$V_{l\text{-}l}$	220	*Volt*
8.	*frekuensi*	50	*Hz*
9.	*Pole*	4	*Unit*
10.	$Rpm_{nominal}$	1500	*Rpm*

B. *Determination of PSO parameters*

PSO is a search algorithm fast in convergence but prone to getting stuck at optimal locales. Therefore, determining appropriate ranges for Kp, Ki, and Kd values before starting the automatic tuning process is essential. The procedure involves setting arbitrary ranges for parameter values and then executing automatic tuning using PSO in the simulation program. Run the tuning with varying reference speeds to observe the convergence patterns of parameter values. This research tested PID tuning with the Kp 0-50, Ki 0-50, and Kd 0-0.05. This yielded the results of the PSO-free parameter testing.

The data obtained from the PSO-free parameter testing represents all individuals who passed the speed characterization test using PSO. This data reveals that the convergent PID range is Kp = 5-15, Ki = 7-15, and Kd = 2m-15m, with each reference speed having over 50% of data passing (green color) within that range. This range will then be used to establish the PID tuning range to avoid the local optima of the PSO method.

C. *LabView Simulation Results*

Based on the LabView simulation program, the results of tuning the PID algorithm PID values are shown in Figure 4 in the Global Best blue panel. PID parameter values of the PSO algorithm at a reference speed of 1500 Rpm without load are Kp = 13, Ki = 11, and Kd = 8.4m, as shown in Figure 7(a). The speed response from the simulation results recorded a reference speed value of 1500 Rpm, which represents the nominal speed, the maximum speed of 1500 Rpm, no-load testing, 2.8 ms dead time, 3.31 ms rise time, and 0% steady error. Figure 7(b) shows the speed response of the PID results without the PSO algorithm.

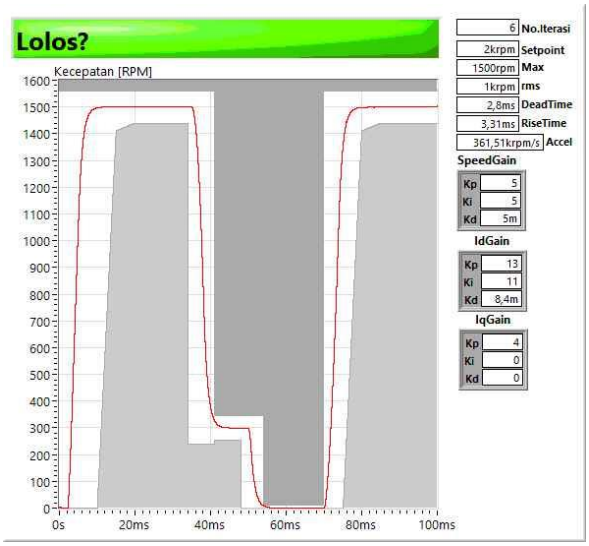

(a)

R. Akbar Nur Apriyanto, Mohammad Erik Echsony, R. Gaguk Pratama Yudha, Adiratna Ciptaningrum, Wahyu Pribadi, Rahayu Mekar Bisono, and Dwi Adhim Zuhli Atmaja, “Simulation of 3 Phase Train Drive Traction Motor Control System for Developing Green Energy Technology and Improving Train Drive System Performance,” *International Research Journal of Advanced Engineering and Science*, Volume 8, Issue 4, pp. 33-40, 2023.

International Research Journal of Advanced Engineering and Science
ISSN (Online): 2455-9024

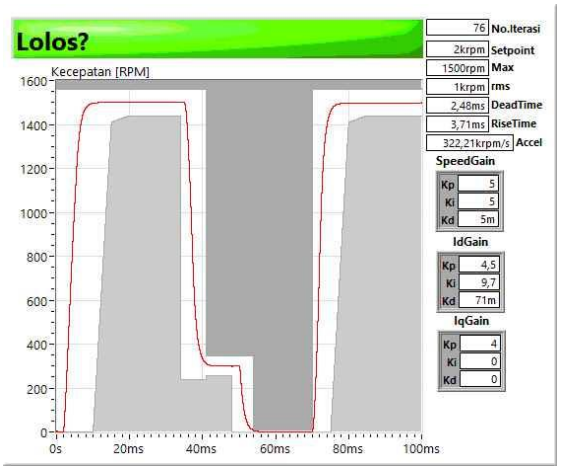

(b)

Fig. 5. PID-PSO tuning result mold speed 1500 RPM, 0 Nm.

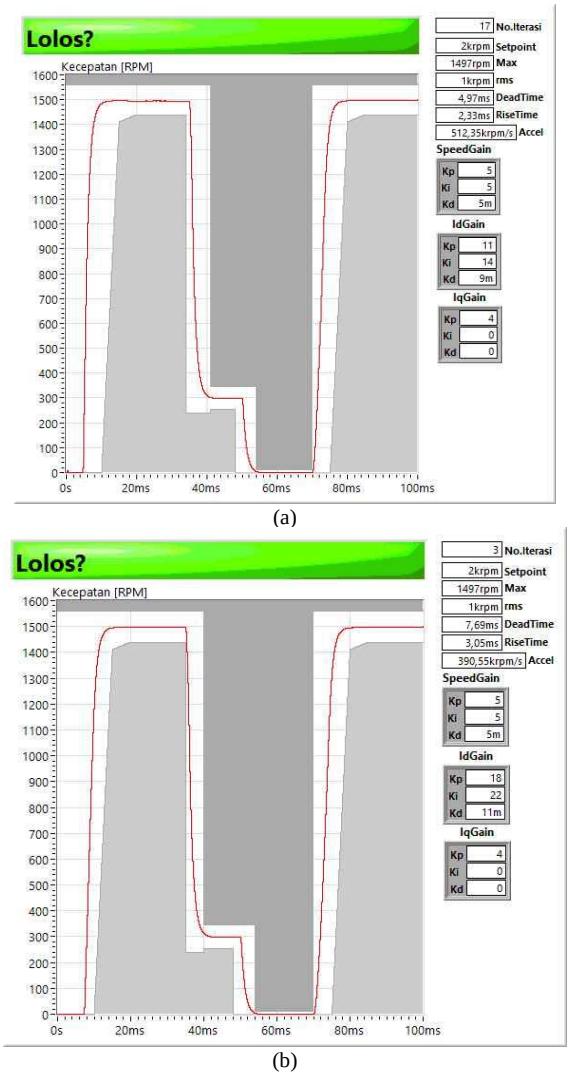

(a)

(b)

Fig. 6. PID-PSO tuning result mold speed 1500 RPM, 3 Nm

Furthermore, the parameter values at the reference speed of 1500 Rpm with a load of 3 Nm obtained the PID parameter values of the PSO algorithm, namely Kp = 11, Ki = 14, and Kd = 9m, as shown in Figure 8(a). The speed response from the simulation results recorded a reference speed value of 1500 Rpm, which represents the nominal speed, the maximum speed of 1497 Rpm, testing with a load of 3 Nm, dead time of 4.97ms, rise time of 2.33 ms and steady error of 0.2%. The PID parameter values without the PSO algorithm at a reference speed of 1500 Rpm with a load of 3 Nm are Kp = 18, Ki = 22, and Kd = 11m, as shown in Figure 8(b). The speed response from the simulation results recorded a reference speed value of 1500 Rpm, which represents the nominal speed, a maximum speed of 1497 Rpm, testing with a load of 3 Nm, dead time of 7.69 ms, rise time of 3.05 ms, and steady error of 0.2%. The value of the PID parameter without the PSO algorithm at a reference speed of 1500 Rpm with a load of 3 Nm is Kp = 18, Ki = 22, and Kd = 11m, as in Figure 8(b). The speed response from the simulation results recorded a reference speed value of 1500 Rpm, which represents the nominal speed, the maximum speed of 1497 Rpm, testing with 3 Nm load, 7.69 ms dead time, 3.05 ms rise time, and 0.2% steady error.

Figure 9 (a) shows the phase current performance of the motor using the PID parameter value generated from the PSO algorithm, (b) shows the phase current performance of the motor using the PID parameter value generated without the PSO algorithm when operated at a speed of 1500 rpm 3 Nm. In measuring the value of the RMS phase current, the PID without the PSO Id current regulator consumes 2.44 A while the PID-PSO consumes 2.41 A. Meanwhile, the performance of the phase current after the FFT for this speed reference is shown in Figure 10 (a) PID-PSO and (b) PID without PSO. PID-PSO produces a THD of 19.41%, while PID without PSO produces a THD of 20.59%. Power consumption from a reference speed of 1500 rpm with a 3 Nm load on the PID-PSO is 828.6 Watts, while for PIDs without PSO, it is 878.2 Watts. The PID-PSO fundamental current is 1.8 A, and the PID fundamental current without PSO is 1.85 A. At 1500 rpm the load is 3 Nm.

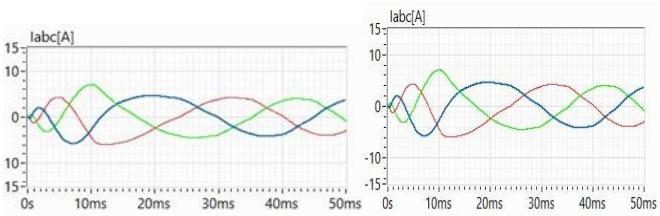

(a) (b)

Fig. 7. (9a) Motor phase current performance PID-PSO parameter reference speed 1500 RPM, 3 Nm. (9b) PID parameter motor phase current performance without PSO reference speed 1500 RPM, 3 Nm

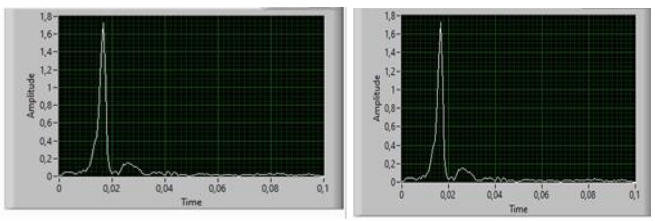

(a) (b)

Fig. 8. (10a) Phase current performance after parameter FFT PID-PSO reference speed 1500 RPM, 3 Nm. (10b) Phase current performance after parameter FFT without PSO reference speed 1500 RPM, 3 Nm

R. Akbar Nur Apriyanto, Mohammad Erik Echsony, R. Gaguk Pratama Yudha, Adiratna Ciptaningrum, Wahyu Pribadi, Rahayu Mekar Bisono, and Dwi Adhim Zuhli Atmaja, “Simulation of 3 Phase Train Drive Traction Motor Control System for Developing Green Energy Technology and Improving Train Drive System Performance,” *International Research Journal of Advanced Engineering and Science*, Volume 8, Issue 4, pp. 33-40, 2023.

International Research Journal of Advanced Engineering and Science
ISSN (Online): 2455-9024

Furthermore, the parameter values at the reference speed of 1500 Rpm with a load of 5 Nm obtained the results of the PID parameter values of the PSO algorithm, namely Kp = 14, Ki = 10, and Kd = 8.3m, as shown in Figure 11(a). The speed response from the simulation results recorded a reference speed value of 1500 Rpm, which represents the nominal speed, a maximum speed of 1495 Rpm, testing with a load of 5 Nm, dead time of 9.32ms, rise time of 3.27 ms and steady error of 0.2%. The PID parameter values without the PSO algorithm at a reference speed of 1500 Rpm with a load of 5 Nm are Kp = 5.6, Ki = 6, and Kd = 9.5m, as shown in Figure 11(b). The speed response from the simulation results recorded a reference speed value of 1500 Rpm, which represents the nominal speed, the maximum speed of 1493 Rpm, testing with a load of 3 Nm, dead time of 9.72 ms, rise time of 2.56 ms, and steady error of 0.2%.

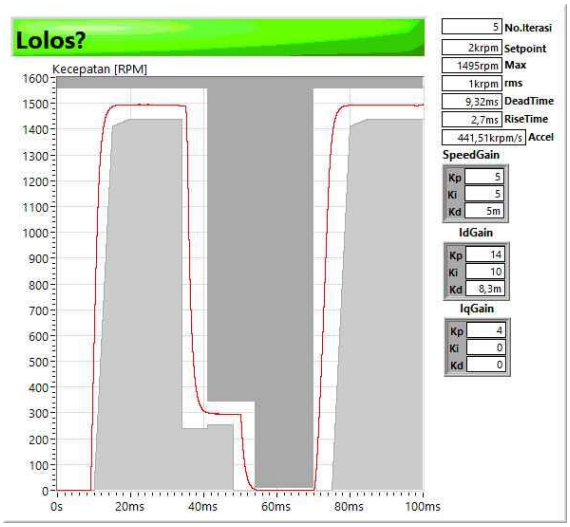

(a)

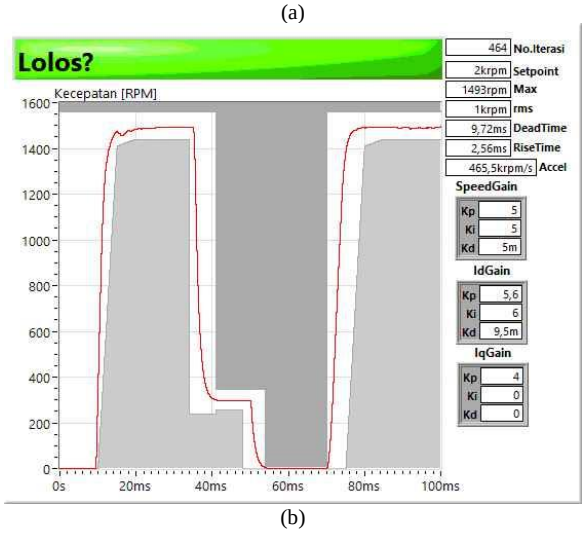

(b)

Fig. 9. PID-PSO tuning result mold speed 1500 RPM, 5 Nm

Figure 12 (a) shows the phase current performance of the motor using the PID parameter value generated from the PSO algorithm, (b) shows the phase current performance of the motor using the PID parameter value generated without the PSO algorithm when operated at a speed of 1500 rpm 5 Nm. In the measurement of the RMS phase current value, PID without the PSO Id current regulator consumes 3.52 A while the PID-PSO consumes 3.49 A. While the phase current performance after FFT for this speed reference is shown in Figure 13 (a) PID-PSO and (b) PID without PSO. PID-PSO produces a THD of 22.71%, while PID without PSO produces a THD of 24.02%. Power consumption from a reference speed of 1500 rpm with a 5 Nm load on the PID-PSO is 1,050 Watts, while for PIDs without PSO is 1,059 Watts. The PID-PSO fundamental current is 2.67 A, and the PID fundamental current without PSO is 2.8 A. At a speed 1500 rpm the load is 5 Nm.

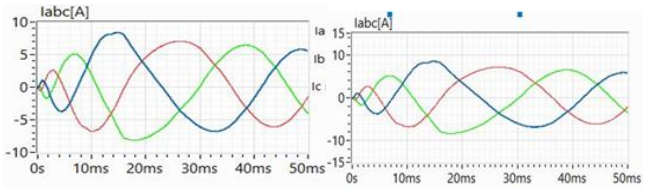

(a) (b)

Fig. 10. (12a) Motor phase current performance PID-PSO parameter reference speed 1500 RPM, 5 Nm. (12b) Motor phase current performance PID parameter without PSO reference speed 1500 RPM, 5 Nm

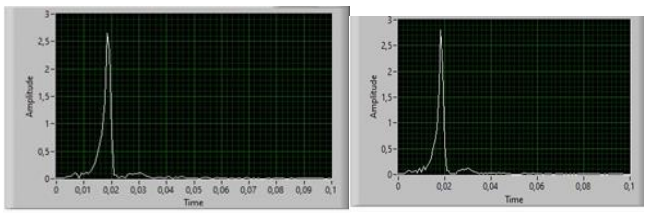

(a) (b)

Fig. 11. (13a) Phase current performance after parameter FFT PID-PSO reference speed 1500 RPM, 5 Nm. (13b) Phase current performance after parameter FFT PID without PSO reference speed 1500 RPM, 5 Nm

TABLE II Simulation results of induction motor current performance

Speed (Load)	Current (A)		Fundamental (A)		THD (%)	
	PSO	Without PSO	PSO	Without PSO	PSO	Without PSO
300 (0)	0,899 A	0,911 A	0,58 A	0,59 A	4,28 %	4,91 %
300 (3)	2,24 A	2,26 A	1,7 A	1,75 A	17,82 %	18,04 %
300 (5)	3,28 A	3,32 A	2,55 A	2,6 A	21,28 %	21, 44 %
800 (0)	0,911 A	0,982 A	0,58 A	0,59 A	7,75 %	9,76 %
800 (3)	2,26 A	2,26 A	1,75 A	1,75 A	18,12 %	18,12 %
800 (5)	3,32 A	3,52 A	2,6 A	2,8 A	22,07 %	23,04 %
1500 (0)	0,985 A	1,00 A	0,62 A	0,8 A	12,33 %	12,62 %
1500 (3)	2,41 A	2,44 A	1,8 A	1,85 A	19, 41 %	20,59 %
1500 (5)	3,49 A	3,52 A	2,67 A	2,8 A	22,71 %	24,02 %

Based on Table 3 displays a current performance evaluation simulation using the implementation induction motor parameters with the PID parameter values obtained in Table 3. It can be seen that, in fact, the current performance results of the PSO algorithm and without PSO are not much

R. Akbar Nur Apriyanto, Mohammad Erik Echsony, R. Gaguk Pratama Yudha, Adiratna Ciptaningrum, Wahyu Pribadi, Rahayu Mekar Bisono, and Dwi Adhim Zuhli Atmaja, “Simulation of 3 Phase Train Drive Traction Motor Control System for Developing Green Energy Technology and Improving Train Drive System Performance,” *International Research Journal of Advanced Engineering and Science*, Volume 8, Issue 4, pp. 33-40, 2023.

different; it's just that the simulation to get the PID value, without PSO is relatively long compared to using PSO.

TABLE III. Evaluation of power and efficiency of induction motors

Speed (Load)	Pin (Watt)		Pout (Watt)		Efficiency (%)	
	PSO	Without PSO	PSO	Without PSO	PSO	Without PSO
300 (0)	249	255	205,5	208,2	82,5%	81,64%
300 (3)	785	823	674,3	680,3	85,8%	82,66%
300 (5)	1063	1150	987,3	999,42	92,8%	86,90%
800 (0)	249,43	274,2	208,2	224,5	83,4%	81,88%
800 (3)	781,41	818,45	680,3	680,3	87,0%	83,12%
800 (5)	1130,7	1217,9	999,4	1059,6	88,4%	87,04%
1500 (0)	264,5	276,3	225,2	228,6	85,1%	82,71%
1500 (3)	828,6	878,2	725,4	734,5	87,5%	83,63%
1500 (5)	1180,5	1201,3	1050,6	1059,6	89,0%	88,25%

Based on Table 4 displays power and efficiency simulations using implementation induction motor parameters with PID parameter values that have been obtained in Table 4. There is a difference in the output power between the PSO algorithm and without PSO, but not too significant. PSO algorithm efficiency and random PID above 80% can be categorized as good.

IV. CONCLUSION

Based on the research that we have carried out in the field, the results of the PID tuning simulation using the Particle Swarm Optimization (PSO) algorithm in LabView for regulation of d-axis stator currents that focus on the performance of induction motor control whose entire system is validated through LabView. PID tuning results of the PSO algorithm can be ascertained to have good results because of the determination of the correct parameter values. The range of PID parameter values in tuning using the PSO algorithm are Kp = 5-15, Ki = 7-15, and Kd = 2-15m. Each change in the speed reference will change the value of Global Best from PSO tuning. Rise time and dead time at speeds of 100 RPM and 1500 RPM do not differ much. At a speed of 1500 RPM, it produces a steady error of 0.5%. Stator current setting d-axis resulting in good speed and efficiency performance. Therefore, in the future, the authors are optimistic that the simulation results of the PID parameter values of the PSO results can be implemented in hardware.

REFERENCES

[1] A, Khichada Bhavin. 2016. "3-Phase Induction Motor Parameter Monitoring and Analysis Using Labview." *International Journal of Electrical Engineering & Technology (IJEET)* 7(6):81–91.

[2] Ali, Jamal Ali, M. A. Hannan, and Azah Mohamed. 2014. "PSO Algorithm for Three Phase Induction Motor Drive with SVPWM Switching and V/f Control." *Conference Proceeding - 2014 IEEE International Conference on Power and Energy, PECon 2014* (1):250–54. doi: 10.1109/PECON.2014.7062451.

[3] Chao, Kuei Hsiang, Yu Sheng Lin, and Uei Dar Lai. 2015. "Improved Particle Swarm Optimization for Maximum Power Point Tracking in Photovoltaic Module Arrays." *Applied Energy* 158:609–18. doi: 10.1016/j.apenergy.2015.08.047.

[4] Nhizanth, A. Ganesan R., and S. Kamban Gopalakrishnan. 2015. "Stepper Motor Control Using LabVIEW and NI-MyRIO Saranathan College of Engineering Trichy , India." 2(12):478–80.

[5] Ramli, Liyana, Yahaya Md Sam, Zaharuddin Mohamed, M. Khairi Aripin, M. Fahezal Ismail, and Liyana Ramli. 2015. "Composite Nonlinear Feedback Control with Multi-Objective Particle Swarm Optimization for Active Front Steering System." *Jurnal Teknologi* 72(2):13–20. doi: 10.11113/jt.v72.3877.

[6] Reza, C. M. F. S., Md Didarul Islam, and Saad Mekhilef. 2014. "A Review of Reliable and Energy Efficient Direct Torque Controlled Induction Motor Drives." *Renewable and Sustainable Energy Reviews* 37:919–32. doi: 10.1016/j.rser.2014.05.067.

[7] Salem, Fawzan, Mohamed A. Awadallah, and Ehab H. E. Bayoumi. 2015. "Model Predictive Control for Deadbeat Performance of Induction Motor Drives." 14(October):303–11.

[8] Suetake, Marcelo, Ivan N. Da Silva, and Alessandro Goedtel. 2011. "Embedded DSP-Based Compact Fuzzy System and Its Application for Induction-Motor V/f Speed Control." *IEEE Transactions on Industrial Electronics* 58(3):750–60. doi: 10.1109/TIE.2010.2047822.

[9] Bazzi, A. M and Krein, P. T. 2010 "Review of Methods for Real-Time Loss Minimization in Induction Machines," *IEEE Transactions on Industry Applications*, vol. 46, no. 6, pp. 2319-2328.

[10] Ferdiansyah, I., Rusli, M. R., Praharsena, B. Toar, H., Ridwan and Purwanto, E. 2018. "Speed Control of Three Phase Induction Motor Using Indirect Field Oriented Control Based on Real-Time Control System," in 2018 10th International Conference on Information Technology and Electrical Engineering (ICITEE), Bali.

[11] Husain, S. and M. A. Bazaz, M. A. 2015. "Review of vector control strategies for three phase induction motor drive," in 2015 *International Conference on Recent Developments in Control, Automation and Power Engineering (RDCAPE)*, Noida.

[12] Purwanto, E., Prabowo, G., Wahyono, E., Rifadil, M. M. 2011. " Pengembangan Model Motor Induksi Sebagai Penggerak Mobil Listrik dengan Menggunakan Metode Vektor Kontrol " *JURNAL ILMIAH ELITE ELEKTRO*, vol. 2, no. 2, pp. 67-72.

[13] Briz, F., Diez, A., Degner, M. W. and Lorenz, R. D. 2001. "Current and flux regulation in field-weakening operation [of induction motors]," *IEEE Transactions on Industry Applications*, vol. 37, no. 1, pp. 42-50.

[14] Briz, F., Diez, A., Degner, M. W. and Lorenz, R. D. 2001. "Current and flux regulation in field-weakening operation [of induction motors]," *IEEE Transactions on Industry Applications*, vol. 37, no. 1, pp. 42-50.

[15] Hannan, M. A., Ali, J. A., Mohamed, A., & Hussain, A. 2018. "Optimization techniques to enhance the performance of induction motor drives: A review." *Renewable and Sustainable Energy Reviews*, 81, 1611–1626.

[16] Fakhruddin, H. H.,Toar, H.,Purwanto, E., Oktavianto, H., Apriyanto, R. A. N., Aditya, A. W. 2020. "Implementasi MyRIO pada Kendali Kecepatan Motor Induksi 3 Fase dengan Berbasis Particle Swarm Optimization (PSO)." *JURNAL ELKOMIKA ITENAS*, Vol. 8, No. 3.

[17] Purnata, H., Risdhayanti, A. D., Putri, S. A., and Komarudin, A. 2017. "Penerapan Metode Hysteresis Space Vector Pulse Width Modulation Pada Inverter Tiga Fasa Untuk Pengaturan Kecepatan Dan Efisiensi Motor Induksi," *Jurnal Inovtek Polbeng*, vol. 7, no. 2, pp. 111-118.

[18] Braslavsky, I., Ishmatov, Z., Plotnikov, Y., and Averbakh, I. 2006. "Energy consumption and losses calculation approach for different classes of induction motor drives," in *International Symposium on Power Electronics, Electrical Drives, Automation and Motion*. SPEEDAM, Taormina.

[19] Quang, N. P., and Dittrich, J. -A. 2015. "Vector Control of Three-Phase AC Machines System Development in the Practice." *New York Dordrecht London*: Springer.

[20] Apriyanto, R. A. N., Purwanto, E., Oktavianto, H., Prabowo, G., Fakhruddin, H. H., Toar, H. 2020. "Kontrol Skalar Dengan Penala Parameter PID Otomatis Menggunakan Algoritma PSO Sebagai Pengendali Kecepatan Motor Induksi Tiga Fasa Berbasis LabView " *JURNAL SAINS TERAPAN POLTEKBA*, Vol. 6, No. 1.